Investigating Bias of DCFT, DPT and Promoted DPT Methods in terms of Phase Parameters Estimation of Chirp Signal

Nooshin Rabiee[1], Hamid Aazad[1*], Naser Parhizgar[1]
1- Department of Electrical Engineering, Shiraz Branch, Islamic Azad University, Shiraz, Iran.
Email: azad@shirazu.ac.ir (Corresponding author)

Received: October 2020 Revised: January 2021 Accepted: March 2021

ABSTRACT:
Amongst the approaches proposed to estimate parameters of a chirp signal sequentially, i.e., the central frequency and the chirp rate, algorithms, such as Discrete Polynomial-Phase Transform (DPT) and promoted DPT, exhibit acceptable estimation accuracy. Algorithms intended to estimate phase parameters sequentially, diminish the order of polynomials in complex exponential power to lower-order polynomials, and then estimate these two parameters using the NLS method in a given single exponential mode. The NLS method, which uses FFT to decrease the computational load of frequency domain search, encounters predicaments. In this work, we assessed the bias of algorithms intended for estimating of phase parameters sequentially using the RBF method. The results of investigating the bias of estimators indicated the improved accuracy of the DPT and promoted DPT algorithms in estimation using the RBF method instead of NLS and also than DCFT method.

KEYWORDS: Discrete Polynomial-Phase Transform (DPT), Linear Frequency Modulation (LFM), Discrete Chirp Fourier Transform (DCFT).

1. INTRODUCTION

In many telecommunication applications such as mobile communications, radar, sound navigation ranging (Sonar) and etc., the transmitted signal is regarded as a chirp signal. In all of these applications, it is significant to accurately estimate the parameters of the noisy chirp signal from limited noisy samples of discrete signals [1-2]. When there is a linear correlation between time and frequency, the chirp signal is known as a Linear Frequency Modulation (LFM). LFM is characterized by its two main parameters, i.e., the central frequency and the chirp rate. LFM signals are widely used in military communications and various detection systems (radar and sonar) due to their considerable capacity in the frequency domain and, thereby, the feasibility of achieving better resolution. Moreover, higher-order harmonics of the frequency-modulated chirps, which are known as Polynomial Phase Signals (PPS) [3], or non-linear frequency modulated chirps have been used in Synthetic Aperture Radars (SAR) [4], biomedicine [5], radio communications or by marine mammals [6]. The estimation of chirp signal parameters is a topic of interest with a variety of applications. Chirp signals with various parameters have multiple applications in active sonar. The estimation of chirp signal parameters is essential in sonar tracking. Also, SAR systems can produce useful and attractive images in terms of quality, resolution, and separability from different areas of the earth through the transmission, reception, and processing of electromagnetic waves. With the global advancements in surface mapping by SARs, the quality of SAR images captured is ever-increasing. Such imaging is extremely critical due to the accuracy in estimating the parameters of chirp signals to produce the best quality image by SAR image generation algorithms. A general assumption in chirp analysis techniques is that the signal amplitude is constant at any observation time. Methods for estimating mono-component LFM parameters with constant amplitude include the use of maximum likelihood [7], model order reduction techniques [8], ambiguity function [9], phase unwrapping [10], and Wigner-Ville distribution [11]. Multi-component LFM parameter estimation methods work based on combining a frequency-time transform (FTT) such as Wigner-Ville transform with an image processing technique , Monte Carlo methods or Markov chain Monte Carlo, Fractional Fourier

Paper type: Research paper
DOI: https://doi.org/10.52547/mjee.15.3.35
How to cite this paper: N. Rabiee, H. Aazad and N. Parhizgar, **"Investigating Bias of DCFT, DPT and Promoted DPT Methods in terms of Phase Parameters Estimation of Chirp Signal"**, *Majlesi Journal of Electrical Engineering*, Vol. 15, No. 3, pp. 35-44, 2021.

Transform (FrFT), and High Order Ambiguity Function. The estimation of PPS parameters with constant amplitude using the high-order ambiguity function (HAF) [12] is for estimating basic mono-component PPS parameters [3] and for multi-component signals [13]. HAF-based estimation is an iterative process. The methods for estimating chirp signal parameters are generally categorized as follow:

- Methods that estimate the central frequency using the chirp rate from the input signal (e.g., DPT and Promoted DPT methods).
- Methods (such as DCFT) that estimate the chirp signal parameter using defined transform and calculating the input signal transform.

In section 2, we describe RBF and NLS methods in the mono-exponential model for estimating the noisy complex exponential frequency. In section 3, we discuss the algorithms for sequential estimating of the phase parameters (e.g., DPT and promoted DPT) and DCFT methods. In section 4, we analyze the simulation results. Finally, the manuscript is concluded in section 5.

2. RBF AND NLS METHODS IN THE MONO-EXPONENTIAL MODE FOR ESTIMATING THE NOISY COMPLEX EXPONENTIAL FREQUENCY

2.1. NLS Method in the Mono-exponential Mode

Nonlinear Least Squares (NLS) is a criterion where the values of parameters of the signal model are selected to minimize the sum of the squares of the difference between the data and the model. Then, this criterion considers the value of the selected parameters as an estimate of the signal parameters [14]. Suppose the signal model, which is the sum of complex polynomials at time t, can be defined as follow:

$$x(t) = \sum_{k=1}^{p} \alpha_k e^{i(\omega_k t + \varphi_k)} \quad (1)$$

Where, $x(t)$ is the sum of P complex exponential without noise, α_k is the amplitude, ω_k is the angular frequency, and φ_k is the k^{th} initial phase of the mixed exponential. ω_k is in the [-π, π] interval, φ_k is the non-random phase in [-π,π] interval, and $\alpha_k > 0$. y(t) is the input data at time t, resulting from saturated *x(t)* with noise $n(t)$.

$$y(t) = x(t) + n(t) \quad (2)$$

To estimate the complex exponential parameters, we need to minimize function f in Equation (3) based on the unknown parameters of the problem:

$$x(t) = \sum_{k=1}^{p} \alpha_k e^{i(\omega_k t + \varphi_k)} \quad (3)$$

The sinusoidal model specified in Equation (3) shows the smallest sum of squares of the model distance from the observed data $\{y(t)\}_{t=1}^{N}$. When f is a nonlinear function of the parameters $\{y(t)\}_{t=1}^{N}$, the method that defines the unknown parameters by minimizing Equation (3) is called the nonlinear least squares (NLS). The function f in Equation (3) can be rewritten as the vector of Equation (4) to (8):

$$A_k = \alpha_k e^{i\varphi_k} \quad (4)$$

$$a = [A_1, \ldots, A_p]^T \quad (5)$$

$$y = [y(0), \ldots., y(N-1)]^T \quad (6)$$

$$B = \begin{bmatrix} 1 & \cdots & 1 \\ \vdots & \ddots & \vdots \\ e^{iN\omega_1} & \ldots & e^{iN\omega_p} \end{bmatrix} \quad (7)$$

$$f = [y - aB]^H [y - aB] \quad (8)$$

Equation (8) is a vector form of Equation (3), where matrix B is a Vandermonde matrix. P is the number of mixed exponentials and N is the number of input data. With the above definitions, Equation (8) can be rewritten as Equation (9):

$$f = [a - (B^H B)^{-1} B^H y]^H [B^H B][a - (B^H B)^{-1} B^H y] + y^H y - y^H B (B^H B)^{-1} B^H y \quad (9)$$

To minimize f, the value of ω must be chosen so that the third expression of Equation (9) is maximized:

$$\hat{\omega} = arg \max_{\omega} [y^H B (B^H B)^{-1} B^H y] \quad (10)$$

and

$$\hat{a} = (B^H B)^{-1} B^H y|_{\omega=\hat{\omega}} \quad (11)$$

2.2. RBF Method for Estimating Complex Exponential Frequency in Noise

The Random Basis Function (RBF) method attempts to match the input data with the linear combination of the base functions. The base functions have non-linear parameters [15]. This method matches data with random functions by altering parameters based on the interval corresponding to them and then presents the parameter of interest as the estimated value of the unknowns of the problem. If y(t), t=0,1,...,N-1, then the received data and the base function that data can be matched with it are as follows:

$$s[t] = A\emptyset[t;\theta],\ t = 0,1,\ldots,N-1 \quad (12)$$

And unknown $\boldsymbol{\theta} = [\theta_1 \theta_2, \ldots, \theta_p]^T$ is dependent. If this method estimates the frequency f_0 of a complex sine, s [t] will be as follow:

$$s[t] = Aexp(j2\pi f_0 t + \varphi) \quad (13)$$

Where, A is the unknown amplitude and $\theta = [f_0]$ and φ are the initial phases. A and f_0 are calculated by minimizing the following equation:

$$J(A, f_0) = \sum_{n=0}^{N-1} |y[t] - Aexp(j2\pi f_0 t + \varphi)|^2 \quad (14)$$

If the complex sine is summed with a complex white Gaussian noise, the NLS estimator used in Equation (14) will be the maximum likelihood (ML) estimator [15]. The ML estimator first minimizes the equation (14) on the amplitude and then minimizes the resulting equation based on the frequency f_0. The process of estimating the frequency of ML in the presence of a complex exponential is equivalent to finding the frequency corresponding to the maximum value of the periodogram (calculated by FFT) [16]. To have an acceptable frequency estimation, we require a long FFT (which takes a lot of computation).

2.3. RBF Algorithm

For optimal minimization of Equation (14), we first need to minimize the following Equation:

$$\mathrm{J}(\mathrm{A}_1, \mathrm{A}_2) = \mathrm{E}_\theta \left[\sum_{t=0}^{\mathrm{N}-1} \left| \mathrm{y}[t] - \mathrm{A}_1 \phi[t;\theta_1] - \mathrm{A}_2 \phi[t;\theta_2] \right|^2 \right] \quad (15)$$

From this Equation, the two amplitudes $\widehat{\mathrm{A}}_2$ and $\widehat{\mathrm{A}}_1$ are obtained. The data vectors, amplitude, and parameter are defined as follows.

$$\mathrm{y} = [\mathrm{y}(0), \mathrm{y}(1), ..., \mathrm{y}(\mathrm{N}-1)]^{\mathrm{T}},\ \alpha = [\mathrm{A}_1, \mathrm{A}_2]^{\mathrm{T}}, \theta = [\theta_1, \theta_2]^{\mathrm{T}} \quad (16)$$

And

$$\boldsymbol{H}(\theta) = \begin{bmatrix} \emptyset[0{:}\theta_1] & \emptyset[0{:}\theta_2] \\ \emptyset[1{:}\theta_1] & \emptyset[1{:}\theta_2] \\ \vdots & \vdots \\ \emptyset[N-1{:}\theta_1] & \emptyset[N-1{:}\theta_2] \end{bmatrix} \quad (17)$$

Where, $\mathbf{H}(\Theta)$ is a random and complex N×2 matrix and equation (18) is obtained as follows:

$$J(\boldsymbol{A}) = E_\theta[(\boldsymbol{y} - \boldsymbol{H}(\theta)\boldsymbol{a})^H (\boldsymbol{y} - \boldsymbol{H}(\theta)\boldsymbol{a})] \quad (18)$$

To calculate the amplitude a by the complex derivative property:

$$\frac{\partial J(\boldsymbol{a})}{\partial \boldsymbol{a}} = E_\theta \left[\frac{\partial}{\partial \boldsymbol{a}} (\boldsymbol{y} - \boldsymbol{H}(\theta)\boldsymbol{a})^H (\boldsymbol{y} - \boldsymbol{H}(\theta)\boldsymbol{a}) \right] = E_\theta \left[\frac{\partial}{\partial \boldsymbol{a}} \left(-\boldsymbol{H}^H(\theta)\right) (\boldsymbol{y} - \boldsymbol{H}(\theta)\boldsymbol{a})^* \right] = 0 \quad (19)$$

And by solving Equation (19) we will have:

$$E_\theta[\boldsymbol{H}^H(\theta)\boldsymbol{H}(\theta)]\hat{\boldsymbol{a}} = E_\theta^H[\boldsymbol{H}(\theta)]\boldsymbol{y} \quad (20)$$

Given the right side of Equation (20) of Equation (17):

$$E_\theta[\boldsymbol{H}(\Theta)] = \begin{bmatrix} E[\emptyset[0{:}\theta_1]] & E[\emptyset[0{:}\theta_2]] \\ E[\emptyset[1{:}\theta_1]] & E[\emptyset[1{:}\theta_2]] \\ \vdots & \vdots \\ E[\emptyset[N-1{:}\theta_1]] & E[\emptyset[N-1{:}\theta_2]] \end{bmatrix} \quad (21)$$

Suppose θ_1 *and* θ_2 are independent:

$$\mathrm{E}_\theta[\mathrm{H}^{\mathrm{H}}(\theta)\mathrm{H}(\theta)] = \begin{bmatrix} \sum_{t=0}^{\mathrm{N}} \mathrm{E}[|\phi[t;\theta_1]|^2] & \sum_{t=0}^{\mathrm{N}} \mathrm{E}[\phi^*[t;\theta_1]\phi[t;\theta_2]] \\ \sum_{t=0}^{\mathrm{N}} \mathrm{E}[\phi[t;\theta_1]\phi^*[t;\theta_2]] & \sum_{t=0}^{\mathrm{N}} \mathrm{E}[|\phi[t;\theta_2]|^2] \end{bmatrix} \quad (22)$$

The frequency value in the RBF method is considered between -0.5 to 0.5. To find $\mathrm{E}[\emptyset[t;\Theta]]$ using Equations (21) and (22) and to consider a uniform PDF for F_0 in the frequency range $[f_1, f_2]$, Equation (23) is obtained as follow:

$$\begin{aligned} & E[\phi[t;\theta]] = E[\phi[t;F_0]] = E[\exp(j\,2\pi F_0 t + \varphi)] \\ & = \int_{f_1}^{f_2} \exp(j\,2\pi F_0 t + \varphi) P_{F_0}(f_0) df_0 \\ & == \int_{f_1}^{f_2} \exp(j\,2\pi F_0 t + \varphi) \frac{1}{f_2 - f_1} df_0 \\ & = \frac{\sin(\pi B t)}{\pi B n} \exp(j\,2\pi\mu t + \varphi) \end{aligned} \quad (23)$$

Where $\mathrm{B} = f_2 - f_1$ and $\mu = \frac{f_2 + f_1}{2}$ are respectively bandwidth and center of the frequency range. Using equations (20), (22), and (23), we can reach Equation (24), where $\omega_s^{(1)}[t] = \frac{\sin(\pi \mathrm{B}^{(1)} t)}{\pi \mathrm{B}^{(1)} t}$.

$$\begin{bmatrix} \widehat{A}_1 \\ \widehat{A}_2 \end{bmatrix} = \begin{bmatrix} N & \sum_{t=0}^{N-1} \omega_s^2[t] e^{-e^{j\,2\pi(\mu_1^{(1)} - \mu_2^{(1)})t}} \\ \sum_{t=0}^{N-1} \omega_s^2[t]\, \mathrm{e}^{j\,2\pi(\mu_1^{(1)} - \mu_2^{(1)})t} & N \end{bmatrix} \times \begin{bmatrix} \sum_{t=0}^{N-1} y[t]\omega_s^2[t]\, \mathrm{e}^{-j\,2\pi\mu_1^{(1)} t + \varphi} \\ \sum_{t=0}^{N-1} y[t]\omega_s^2[t]\, \mathrm{e}^{j\,2\pi\mu_2^{(1)} t + \varphi} \end{bmatrix} \quad (24)$$

The following algorithm can be considered to estimate the frequency of a complex sine in noise. Suppose the unknown parameter f_0 belongs to the interval $[-a, a]$. In this case, the interval related to the estimated parameter f_0 is split into two equal intervals [15].

Step 1: For the first step of k steps, which is shown with superscript (1), we consider the frequency of the first step as $f_{1_l}^{(1)} = -0.5, f_{u_l}^{(1)} = 0$ and the second frequency interval as $f_{2_l}^{(1)} = 0, f_{2_u}^{(1)} = 0.5$. We select the center of the first and second frequency bands

respectively as $\mu_1 = \frac{-1}{4}$ and $\mu_2 = \frac{1}{4}$. Also, we consider the frequency band terminal as $B^{(1)} = 0.5$.

Step 2: Using Equation (24), we estimate the complex amplitudes of the two frequency bands separately from the previous step.

Step 3: We select the interval with a higher power $\left|A^{(1)}\right|^2$ from the previous two intervals as the new interval and then split it into two separate intervals. In this case, we define $f_{2_l}^{(2)}$, $f_{2_u}^{(2)}$, $f_{1_l}^{(2)}$, $f_{1_u}^{(2)}$, and $\mu_1^{(2)}$، $\mu_2^{(2)}$ $B^{(2)} = \frac{B^{(1)}}{2} = \frac{1}{4}$.

Step 4: We repeat steps 1 and 2 based on the new estimation interval of the third step and considering the upper and lower limits corresponding to the new interval. This will continue until the bandwidth is minimized. The bandwidth reduces by a factor of $\frac{1}{2}$ at each step, thereby, the bandwidth of the last interval is $\frac{1}{2^k}$.

Step 5: After k iterations, the frequency estimate will be:

$$\hat{f_0} = \frac{1}{2}\left(f_u^{(k)} + f_l^{(k)}\right) \quad (25)$$

3. CHIRP SIGNAL PARAMETER ESTIMATION METHODS

The chirp signal model is considered as a complex exponential signal in which the instantaneous frequency of this signal increases linearly with time. The slope of the frequency changes with k_r is shown. The intercept of the instantaneous frequency of this signal is the central frequency carrying f_0. If there is a linear relationship between time and frequency, the chirp signal is known as an LFM. The quadratic relationship between time and frequency leads to the Quadratic Frequency Modulated (QFM) signal. The complex chirp signal model is considered as Equation (26) as:

$$x(t) = ae^{j\left(2\pi\left(0.5\,k_r\,t^2 + f_0\,t\right)\right)}, t = 0, \ldots, N-1 \quad (26)$$

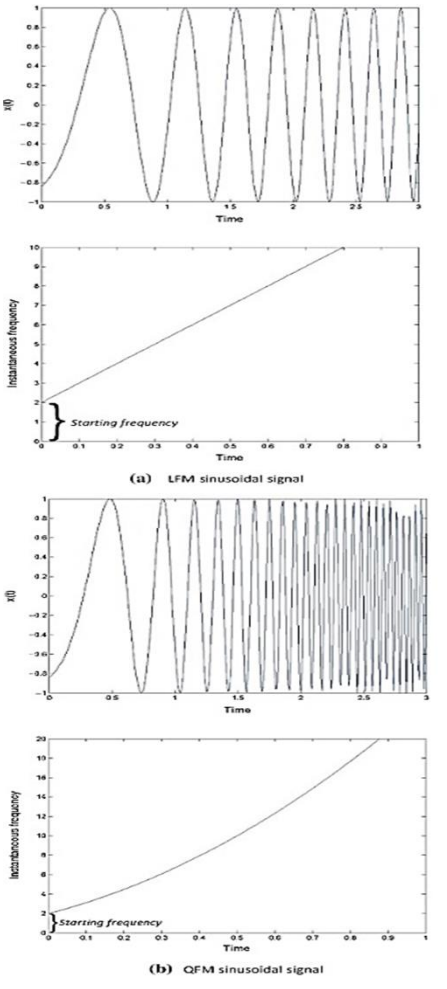

Fig. 1. Illustration of QFM and LFM signal [17].

3.1. Estimation of Phase Parameters Sequentially in Discrete Polynomial Transform (DPT) Method

Algorithms designed to estimate phase parameters sequentially, diminish the order of polynomials in complex exponential power to lower-order polynomials $e^{j\,k_r{}'t + j\varphi}$. Using the NLS method, we can estimate higher-order parameters. Then, we can estimate lower-order parameters by neutralizing the impact of higher-order parameters. This operation continues until all complex exponential parameters were estimated [9]. If the noiseless signal is defined as Equation (26), r(t) can be defined as follows:

$$r(t) = x(t+\tau)\,x^*(t) = A\,e^{j\,2\pi\,(2\times 0.5\times t\times k_r\times\tau)}, t = 0, \ldots, N-1-\tau \quad (27)$$

Where, the complex amplitude A is as $|a|^2 e^{j(f_0\tau + k_r\tau^2)}$, τ is a positive integer, and * represents the conjugate of a complex number. Therefore, we can estimate frequency τk_r using the estimation methods. When the frequency τk_r is

estimated, the demodulated signal of signal $x(t)$ is considered as follows:

$$z(t) = x(t)e^{-j\,2\pi\,(0.5\,\widehat{k_r}\;t^2)} \simeq ae^{j2\pi f_0 t} \tag{28}$$

Where $\widehat{k_r}$ denotes an estimate of the slope of the change in frequency of the chirp signal. The signal z(t) is also a complex exponential signal with frequency f_0 or the central frequency of the chirp signal. If $\widehat{k_r} = k_r$, we can by the generated signal z(t) obtain the parameter f_0 using a frequency estimation method. In the DPT method, the chirp rate is estimated using the NLS method.

3.2. Iteration Algorithm (promoted DPT)

Ikram [18] used an iteration algorithm to improve the estimation accuracy of the parameters k_r and f_0. The iteration algorithm consists of two steps. The first step is to estimate the parameter k_r and improve its accuracy using consecutive iterations and the second step is to estimate the parameter f_0.

Step 1: Consider the following definition:

$$r_k(t) = w_{k-1}(t+\tau_{k+1})w^*_{k-1}(t),\ t = 0,1,...,N-1-\tau_{k-1} \tag{29}$$

Where, w_{k-1} is also defined as follows:

$$w_{k-1}(t) = y(t)e^{-j\,2\pi(0.5\hat{k}_{r_{k-1}}t^2)},\quad t = 0,1,...,N-1 \tag{30}$$

Where, the parameter k represents the kth iteration of the first step. For the first iteration (k = 1), the initial value of $\widehat{k_r} = 0$ and $\tau = 1$ is selected. Therefore, in the first iteration, Equation (29) will be as follows:

$$r_1(t) = y(t+\tau_0)\,y^*(t),\ \ t = 0,\dots,N-1-\tau_0 \tag{31}$$

Which leads to the estimation of the parameter $\widehat{k_{r\,1}}$. In the second and higher iterations (k = 2, …), the demodulated signal $w_{k-1}(t)$ is as a chirp signal with central frequency f_0, and the slope of variation in the chirp signal frequency is as $\Delta k_{rk-1} = k_r - \widehat{k_{r_{k-1}}}$. We can estimate the value of Δk_{rk-1} using $r_k(t)$. The improved value of the k_r estimation is as follows:

$$\widehat{k_{rk}} = \Delta k_{r_{k-1}} + \widehat{k_{r_{k-1}}} \tag{32}$$

When the value of $|\Delta k_{r_{k-1}}|$ is too small (or after a certain number of iterations), the first step stops. To avoid ambiguity in the first step, the value of τ starts with small values such as ($\tau = 1$). After estimating the parameter k_r with acceptable accuracy, we estimate the parameter f_0 using the signal z(t) in Equation (28). After estimating the parameters k_r and f_0, we can estimate the signal amplitude as follows:

$$\begin{aligned}\hat{a} &= \arg\min_a \sum_{t=0}^{N-1}\left|y(t) - ae^{j(2\pi(0.5k_r t^2 + f_0 t))}\right|^2 \\ &= \frac{1}{N}\sum_{t=0}^{N-1}\left|y(t)e^{j(2\pi(0.5\hat{k}_r t^2 + \hat{f}_0 t))}\right|^2\end{aligned} \tag{33}$$

3.3. DCFT Method

The second-order chirp signal is a non-stationary signal. In SAR imaging, when the targets are moving at a constant speed, the signal transmitted from these targets is a second-order chirp signal. Signals returned from these targets on the radar contain essential information about mobile targets such as speed and location. In the second-order chirp signal, besides the central frequency, the chirp rate is also available, and the DFT matches the multi-harmonic frequency. Using DFT transform, we can efficiently estimate the harmonics of stationary signals, but for non-stationary signals, such as chirps, DFT will perform very poorly due to considerable variations in the frequency characteristics of these types of signals with the time. Therefore, we often use Discrete Chirp-Fourier Transform (DCFT) to process non-stationary signals (especially chirps). DCFT transform is a generalization of DFT transform that can help us to obtain the chirp rate of discrete-time signals with an acceptable approximation. The DCFT method is the extension of the DFT transform for the chirp signal and is used to estimate the central frequency parameters and the chirp rate. In DFT transform, if the input signal is a combination of several sinusoidal components, the DFT output will contain peaks at the same frequencies corresponding to the input signal harmonics. DFT transform of a discrete signal is as follows:

$$X(k) = \frac{1}{\sqrt{N}}\sum_{n=0}^{N-1}x(n)W_N^{kn},\quad 0 \le k \le N-1 \tag{34}$$

Where, $W_N^{kn} = e^{-j\omega_0}$, and DCFT transform is defined by a similar equation as follows:

$$X_c(k,l) = \frac{1}{\sqrt{N}}\sum_{n=0}^{N-1}x(n)W_N^{ln^2+kn},\quad 0 \le k,l \le N-1 \tag{35}$$

The parameters k and l represent constant frequencies and chirp rates, respectively. The DCFT of signal $x(n)$ is the same as the DFT of signal $x(n)W_N^{ln^2}$, and for $l = 0$, the DCFT of signal $x(n)$ will be equal to its DFT. For extraction of the two parameters (harmonic frequency and chirp rate), we need a 3D plot of the function $X_c(k,l)$ obtained from the DCFT definition equation at values of k and *l*. Also, we should save the values of k and *l* as the response (desired estimation) from points where peaks have occurred. In [19], a particular example is given to illustrate the DCFT transform performance when the input signal is

a combination of two integrated chirp signals. Fig. 2 shows the output power spectrum of the DCFT transform in terms of frequency and Doppler rate in the form of a 3D function. The values of harmonic frequency and chirp rate (parameters k and *l* in the previous equations) were respectively 42 and 15 (for the first signal) and 45 and 44 (for the second signal), indicating that these two signals are merged (normal sum). Also, the SNR of these two signals is respectively 0 and 6dB. In Fig. 2, the DCFT output power spectrum has two peaks, showing the same coordinates of the two combined chirp signals. Fig. 2 confirms the high accuracy of DCFT estimation.

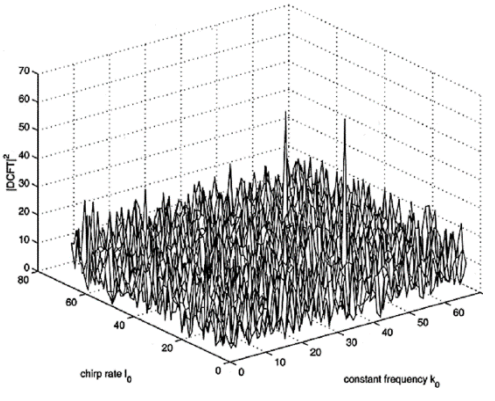

Fig. 2. DCFT output power spectrum in a specific mode by combining two chirp signals [19].

4. SIMULATION RESULT

Algorithms intended to estimate phase parameters sequentially, diminish the order of polynomials in complex exponential power to lower-order polynomials. Using the NLS method, we can estimate higher-order parameters. Then, lower-order parameters are estimated by neutralizing the impact of higher-order parameters. The NLS method in the mono-exponential mood is the same as the periodogram method. The promoted DPT method improves the accuracy of the DPT chirp rate using an iterative algorithm with accessible data. In the DPT and promoted DPT methods, the central frequency and the chirp rate at each step are calculated by the periodogram method. The periodogram method, which uses FFT to diminish the computational load of frequency domain search, comes with some restrictions such limited amount of Mean Squared Error (MSE) for the estimated frequency and the high rate of calculations than other methods proposed for estimating frequency. Therefore, in [20], the idea of using another method for frequency estimation to enhance the accuracy of DPT and promoted DPT algorithms is presented. Thereby, the estimation accuracy can be increased by using the RBF method instead of the NLS [20-22]. In these simulations, 10,000 experiments are conducted independently, and the inverse MSE of the estimation of the parameters in these simulations at different SNRs are compared with the inverse CRLB criterion. The number of accessible samples is 20, the central frequency is 0.3, and the chirp rate is 0.2. The length of FFT for the implementation of NLS and DCFT methods is 128. Figs. 3 and 4 show the performance of NLS-DPT, DPT-RBF, and DCFT methods for estimating phase parameters of the chip signal [20-22].

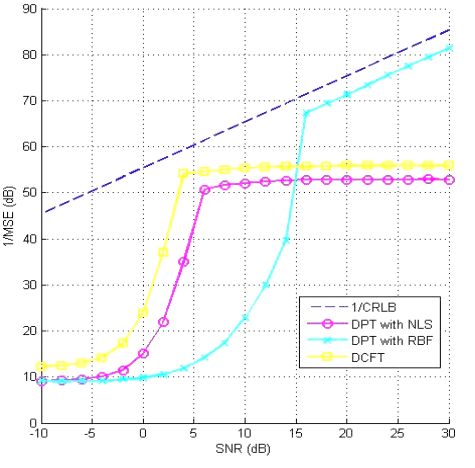

Fig. 3. MSE inverse versus SNR for chirp rate estimation in different SNR by DPT with NLS, DCFT, and DPT with RBF methods.

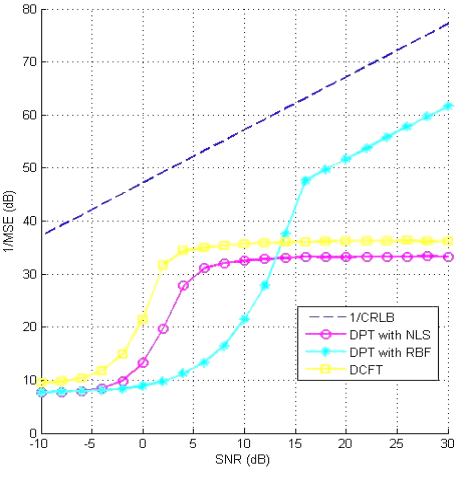

Fig. 4. MSE inverse versus SNR for central frequency estimation in different SNR by DPT with NLS, DCFT, and DPT with RBF methods.

Figs. 5 and 6 show the performance of the promoted DPT-NLS and promoted DPT-RBF methods for estimating the chip phase signal parameters with a chirp rate of 0.2 and a central frequency of 0.3.

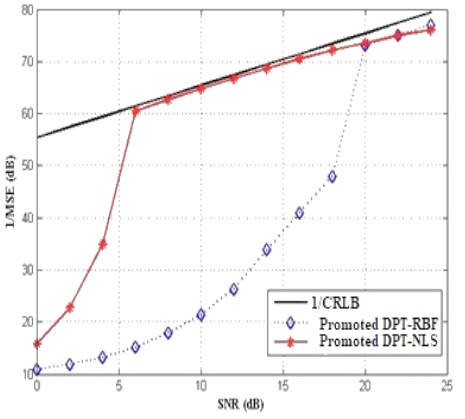

Fig. 5. MSE inverse versus SNR for chirp rate estimation in different SNR using Promoted DPT-NLS and Promoted DPT- RBF methods.

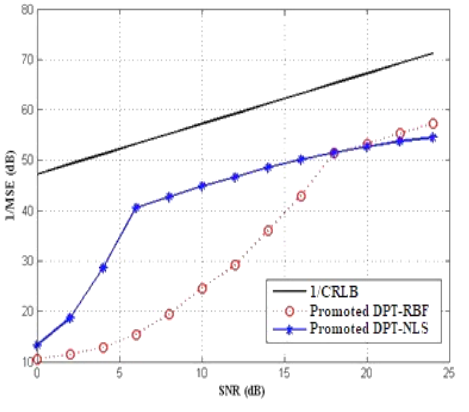

Fig. 6. MSE inverse versus SNR for central frequency estimation in different SNR by Promoted DPT-NLS and Promoted DPT- RBF methods.

The MSE of the DPT method is far from the CRLB criterion. Differently put, this method comes with considerable errors. This problem has been somewhat fixed in the promoted DPT method. The error with estimating the rate of chirp has been decreased in the promoted DPT method. The DPT and promoted DPT with NLS method performs better than the DPT and promoted DPT with RBF method at low SNRs. At high SNRs, the DPT and promoted DPT with RBF estimator performs better than the DPT and promoted DPT with NLS method [20-22]. In the following sections, the bias of the aforementioned estimators is simulated and calculated. Figs. 7 to 18 show the bias of these methods.

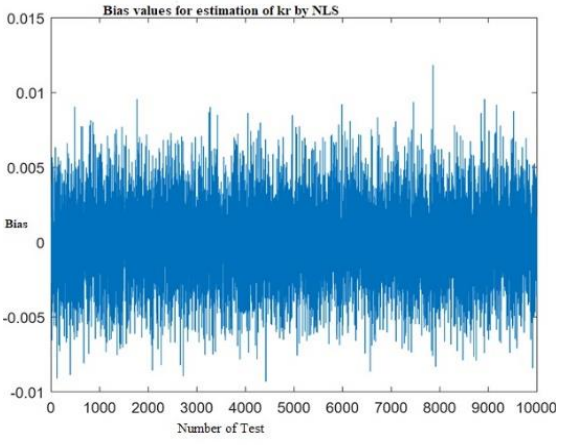

Fig. 7. Bias of NLS estimator for k_r estimation of chirp signal.

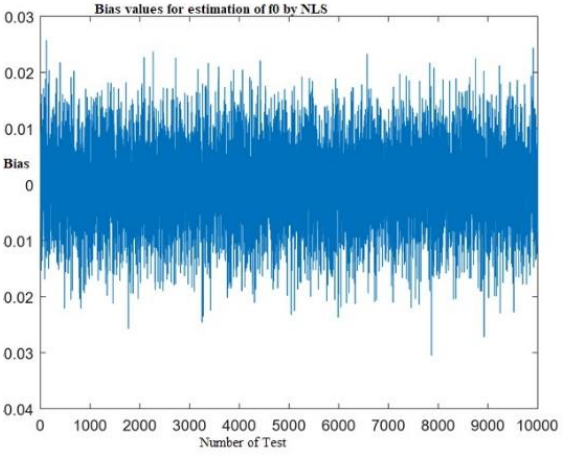

Fig. 8. Bias of NLS estimator for f_0 estimation of chirp signal.

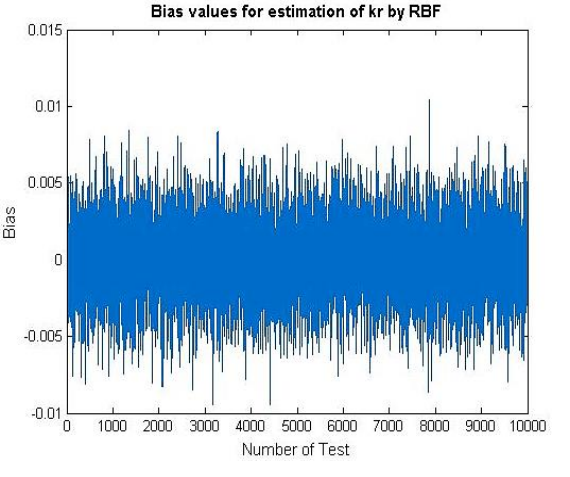

Fig. 9. Bias of RBF estimator for kr estimation of chirp signal.

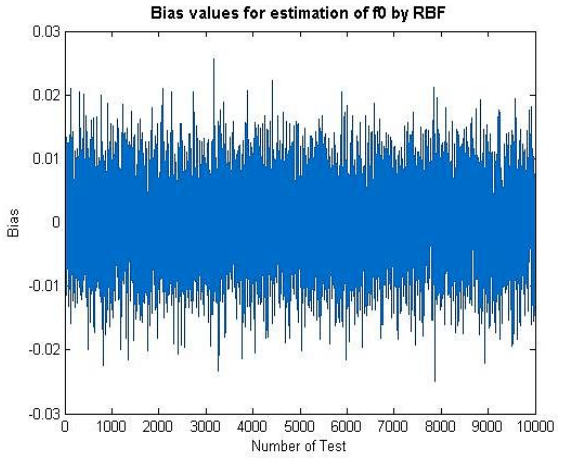

Fig. 10. Bias of RBF estimator for f_0 estimation of chirp signal.

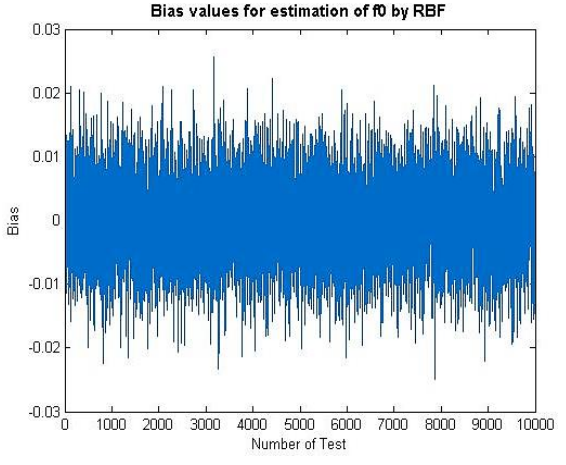

Fig. 11. Bias for k_r estimation of chirp signal in DPT-NLS method.

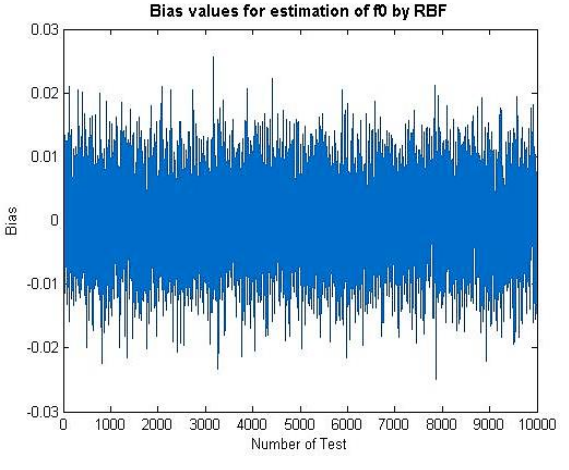

Fig. 12. Bias for f_0 estimation of chirp signal in DPT-NLS method.

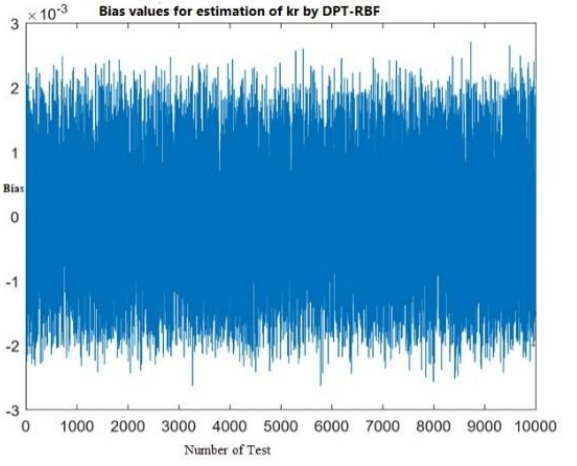

Fig. 13. Bias for f_0 estimation of chirp signal in DPT-NLS method.

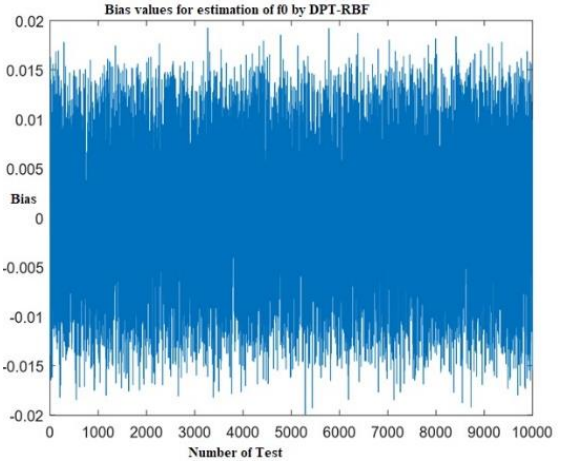

Fig. 14. Bias for f_0 estimation of chirp signal in DPT-NLS method.

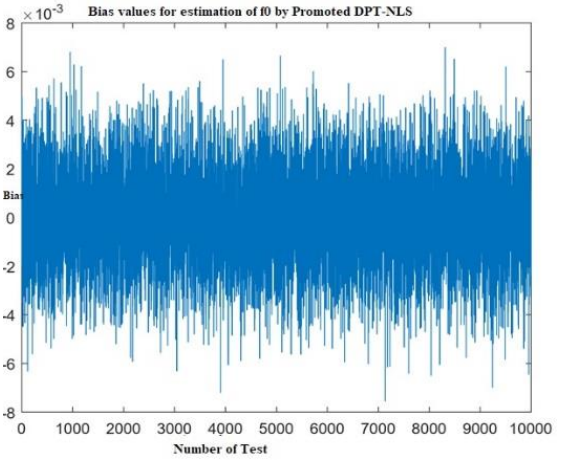

Fig. 15. Bias for k_r estimation of chirp signal in promoted DPT-NLS method.

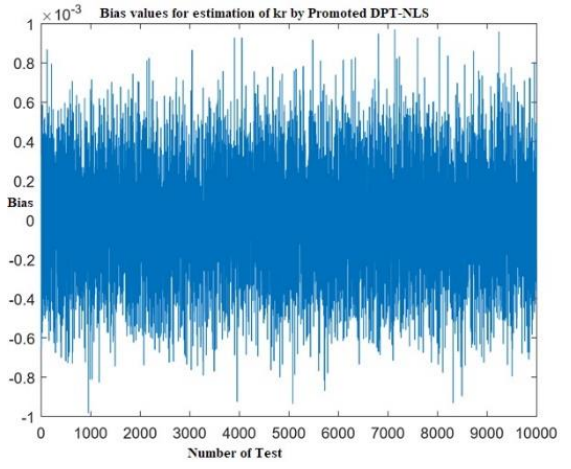

Fig. 16. Bias for f_0 estimation of chirp signal in promoted DPT-NLS method.

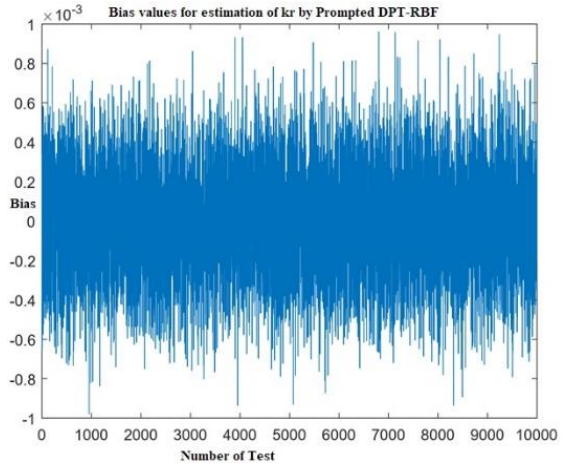

Fig. 17. Bias for f_0 estimation of chirp signal in promoted DPT-NLS method.

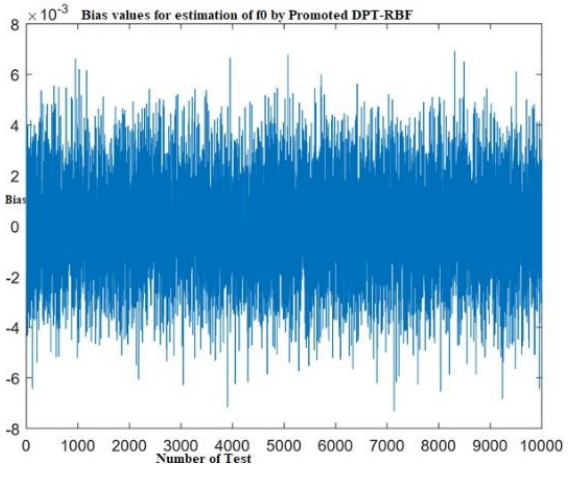

Fig. 18. Bias for f_0 estimation of chirp signal in promoted DPT-RBF method.

Table 1 shows the bias values of the different estimators for estimating the parameters (k_r) and (f_0). To calculate the bias of each estimator, the absolute values of the estimator error were averaged in several experiments (10,000 experiments in these simulations) and the value is shown in Table (1).

Table 1. The bias values of the different estimators for estimating the parameters (k_r) and (f_0).

Method	Bias for estimation of k_r	Bias for estimation of f_0
NLS	3.1395×10^{-5}	8.8959×10^{-5}
RBF	1.3219×10^{-5}	3.7103×10^{-5}
DPT-NLS	1.3347×10^{-5}	2.2316×10^{-5}
DPT-RBF	1.1391×10^{-6}	6.7868×10^{-6}
Promoted DPT-NLS	1.4265×10^{-7}	2.1924×10^{-5}
Promoted DPT-RBF	4.8087×10^{-8}	1.7750×10^{-5}
DCFT	5.6556×10^{-5}	3.5649×10^{-5}

5. CONCLUSION

In this study, we investigated and calculated the bias of the RBF method (instead of the NLS method) in algorithms intended for estimating phase parameters, i.e., DPT and promoted DPT, and compared the results with the results of the DCFT method. As mentioned in the section (4), using the RBF method instead of the NLS in the promoted DPT and DPT methods, the performance of the promoted DPT and DPT methods in high SNRs is developed which these changes are more considerable at higher SNRs. From Table (1), the DPT with RBF and promoted DPT with RBF methods show better performance than the DCFT method due to the less bias.

REFERENCES

[1] S. Chatterjee, S. Dalai, S. Chakravorti, B. Chatterjee , "**Use of chirp excitations for frequency domain spectroscopy measurement of oil-paper insulation**," *IEEE Transactions on Dielectrics and Electrical Insulation*, Vol. 25 ,Issue. 3, pp. 1103 – 1111, June 2018.

[2] S. Sankar Dhar, D. Kundu , Ujjwal Das, "**Tests For the Parameters of Chirp Signal Model**," *IEEE Transactions on Signal Processing*, Vol. 67, Issue. 16, pp. 4291 – 4301, Aug 2019.

[3] Peleg S. Friedlander B, "**The discrete polynomial–phase transform**," *IEEE Transactions on Signal Processing*, Vol. 43, No. 8, pp. 1901–1914, 1995

[4] Perry RP. DiPietro RC. Fante R, "**SAR imaging of moving targets**,"*IEEE Transactions on Aerospace and Electronic Systems*, Vol. 35, No. 1, pp. 188–200, 1999.

[5] Rankine N. Stevenson M. Mesbah M. Boashash B, "**A nonstationary model of newborn EEG**," *IEEE Transactions on Biomedical Engineering*, Vol. 54, No. 1, pp. 19–28, 2007.

[6] Vespe M. Jones G. Baker C, "**Lessons for radar: waveform diversity inecholocating mammals**,"*IEEE Signal Processing Magazine*, Vol. 26, No. 1, pp. 65–75, 2009.

[7] Abatzoglou T J, "**Fast maximum likelihood joint estimation of frequency and frequency rate**," *IEEE Transactions on Aerospace and Electronic Systems*, Vol. 22, No. 6, pp.708–715, 1986.

[8] Volcker B. Ottersten B, "Chirp parameter estimation using rank reduction. Conference Record of Thirty–Second Asilomar Conference on Signals,"*Systems and Computers, Pacific Grove, CA, USA*, pp. 1443–1446, 1998.

[9] Peleg S. Porat B, "**Linear FM signal parameter estimation from discrete–time observations**,"*IEEE Transactions on Aerospace and Electronic Systems*, Vol. 27, No. 4, pp. 607–616, 1991.

[10] Djuric PM. Kay SM, "**Parameter estimation of chirp signals**," *IEEE Transactions on Acoustics, Speech, and Signal Processing*, Vol. 38, No. 12, pp. 2118–2126, 1990.

[11] O'Shea P, "**Fast parameter estimation algorithms for linear FM signals**," IEEE International Conference on Acoustics, Speech and Signal Processing, Adelaide, SA, Australia, pp. 17–20, 1994.

[12] Porat B, "**Digital processing of random signals: theory and methods**," *Prentice Hall Information and System Sciences Series, Englewood Cliffs, NJ, USA: Prentice Hall*, 1994, ISBN: 9780486462981.

[13] M. G. Christensen, L. J. Højvang, A. Jakobsson, and S. H. Jensen, "**Joint fundamental frequency and order estimation using optimal filtering**," *EURASIPJ. Adv. Signal Process*, Vol. 2011, No. 1, pp. 1–18, June 2011.

[14] P. Stoica and R. L. Moses, "**Spectral analysis of signals**," Pearson/Prentice Hall Upper Saddle River, NJ, (2005). ISBN: 0131139568

[15] Kay S, "**Signal fitting with uncertain basis functions**," *IEEE Signal Processing Letters*., Vol. 6, no 18, pp. 383–386, 2011.

[16] Kay SM, "**Fundamentals of Statistical Signal Processing: Practical Algorithm. Development**," Vol. 3. *Pearson Education*, 2013. ISBN: 978–0132808033

[17] Sahay S.B. Meghasyam T. Roy R.K, "Parameter estimation of linear and quadratic chirps by employing the fractional fourier transform and a generalized time frequency transform,"*Indian Academy of Sciences, Sadhan Journal*, Vol. 40, No. 4, pp. 1049–1075, 2015.

[18] Ikram MZ. Abed–Meraim K. Hua Y, "**Estimating the parameters of chirp signals: an iterative approach**," *IEEE Transactions on Signal Processing*, Vol. 46, No. 12, pp. 3436–3441, 1998.

[19] Xiang-Gen Xia, "**Discrete Chirp-Fourier Transform and Its Applicationto Chirp Rate Estimation**," *IEEE Trans. Signal Processing*, VOL. 48, NO. 11, November 2000.

[20] S. Fallah Tafty, M. Karimi, "**Estimating the Frequency of a Complex Exponential and Parameters of Chirp Signal in Noise**," *MSc thesis, Dept. Electron. Eng., Shiraz Univ., Shiraz, Iran*, 2016.

[21] S. Fallah Tafty, M. Karimi, M. Behzad Fallahpour, "**Improvement of the Accuracy and Reduction of the Computational Complexity of the Discrete Polynomial-Phase Transform Method for the Estimation of Chirp Signal Parameters**," *Journal of Radar*, vol. 5, No. 2, 2017.

[22] S. Fallah Tafty, M. Karimi, "**A Combined Method for Estimating the Frequency of a Complex Exponential**," *24th Iranian Conference on Electrical Engineering (ICEE)*, 2016.